HTML ABSTRACT + LINKS

Chip-scale atomic magnetometer

Peter D. D. Schwindt,[a] Svenja Knappe, Vishal Shah,[b] Leo Hollberg, and John Kitching
Time and Frequency Division, National Institute of Standards and Technology, Boulder, Colorado 80305

Li-Anne Liew and John Moreland
Electromagnetics Division, National Institute of Standards and Technology, Boulder, Colorado 80305

(Received 16 August 2004; accepted 18 October 2004)

Using the techniques of microelectromechanical systems, we have constructed a small low-power magnetic sensor based on alkali atoms. We use a coherent population trapping resonance to probe the interaction of the atoms' magnetic moment with a magnetic field, and we detect changes in the magnetic flux density with a sensitivity of 50 pT $Hz^{-1/2}$ at 10 Hz. The magnetic sensor has a size of 12 mm^3 and dissipates 195 mW of power. Further improvements in size, power dissipation, and magnetic field sensitivity are immediately foreseeable, and such a device could provide a hand-held battery-operated magnetometer with an atom shot-noise limited sensitivity of 0.05 pT $Hz^{-1/2}$. [DOI: 10.1063/1.1839274]

Measurement of magnetic fields with picotesla sensitivity is critical to many applications including underground and underwater ordinance detection,[1] geophysical mapping,[2] navigation, and even the detection and mapping of the human heart beat.[3] Sensitive magnetometers often weigh several kilograms, are quite bulky, and dissipate substantial power while operating. In addition, as the sensitivity increases so does the size and power consumption. Large-scale optical magnetometers[4] that use alkali metal vapors achieve sensitivities[5,6] of ~ 1 fT $Hz^{-1/2}$, and rival superconducting quantum interference devices[7] in this regard without the need for cryogenic cooling. Depending on the design of an atom-optical magnetometer, it can operate in a magnetic flux density ranging from 10^{-15} to $>10^{-3}$ T. An optical magnetometer measures the absolute field, thereby needing no external calibration, since the measured spin precession frequency of the alkali atom has a known direct relation to the magnetic flux density. By miniaturizing an optical magnetometer based on the coherent population trapping (CPT) effect[8] by a factor of 10^4, we demonstrate a highly sensitive magnetic sensor that is millimeters in size, and has the potential to enable, for example, long-range remote sensing of magnetic fields based on battery-operated disposable devices.

The magnetic sensor that we have developed (Fig. 1) utilizes the techniques of microelectromechanical systems to enable small size and low-power consumption. The device's design is amenable to wafer-level fabrication in which wafers containing hundreds of each component could be stacked to allow multiple sensors to be assembled simultaneously, potentially reducing the manufacturing costs dramatically. Since the sensor's components are inherently nonmagnetic, it can be used in applications where a field-producing sensor, such as a fluxgate, is unacceptable. This magnetic sensor is closely related in design to a miniature cesium atomic clock we have recently developed.[9] The core of the sensor is a microfabricated rubidium vapor cell that is made by anodically bonding a glass wafer to either side of a 1 mm thick silicon wafer with a 1 mm^2 hole etched through it.[10] The cell is filled with ^{87}Rb and a buffer gas containing a mixture of argon at 11 kPa and neon at 21 kPa that reduces the frequency of decohering Rb-cell-wall collisions. To create sufficient atomic density in the small cell, we heat it to 120 °C by dissipating 160 mW into two transparent indium-tin-oxide (ITO) heaters placed on either side of the cell. The cell is illuminated with a vertical-cavity surface-emitting laser (VCSEL). The light from the VCSEL passes through a micro-optics package that attenuates the power to 5 μW, circularly polarizes the beam, and collimates it to a diameter of 170 μm. After the beam passes through the cell, it is detected by a *p-i-n* silicon photodiode. When all components are stacked together, the sensor is 3.9 mm high and occupies a volume of 12 mm^3 (Fig. 1).

To measure the magnetic flux density experienced by the ^{87}Rb atoms, we probe the $5S_{1/2}$ ground-state hyperfine splitting between two magnetically sensitive Zeeman states via a

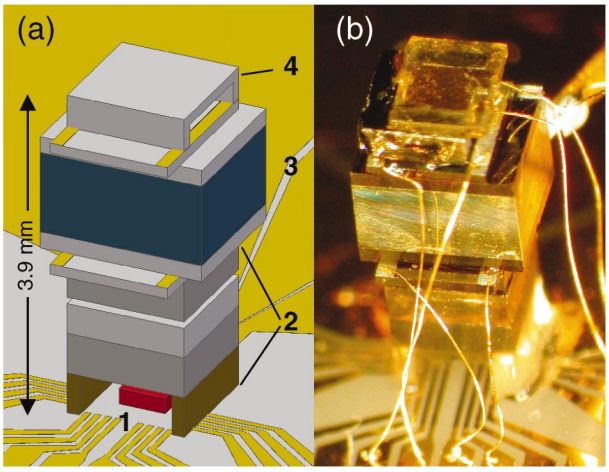

FIG. 1. (Color) The chip-scale atomic magnetometer. (a) Schematic of the magnetic sensor. The components are: 1—VCSEL, 2—optics package including (from bottom to top) a glass spacer, a neutral-density filter, a refractive microlens surrounded by an SU-8 spacer, a quartz $\lambda/4$ waveplate, and a neutral-density filter, 3—^{87}Rb vapor cell with transparent ITO heaters above and below it, and 4—photodiode assembly. (b) Photograph of the magnetic sensor. Note the gold wire bonds providing the electrical connections from the base plate to the ITO heaters and the photodiode.

[a]Electronic mail: schwindt@boulder.nist.gov
[b]Also at: Department of Physics, University of Colorado, Boulder, CO.

Downloaded 30 Dec 2004 to 132.163.52.165. Redistribution subject to AIP license or copyright, see http://apl.aip.org/apl/copyright.jsp

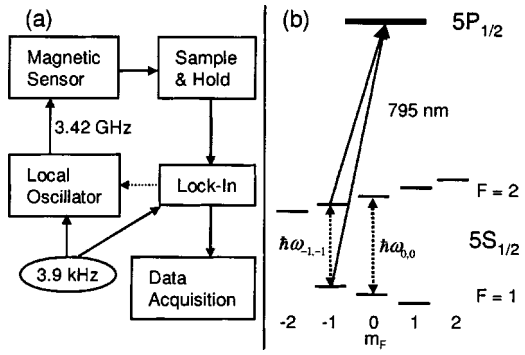

FIG. 2. (a) The experimental setup for detecting the magnetic flux density. The dashed arrow indicates that the lock-in amplifier can provide feedback to the local oscillator, allowing the local oscillator to track large changes in magnetic field. The magnetometer is run open loop for the data in Figs. 3 and 4. (b) Energy level diagram (not to scale) of ^{87}Rb showing the resonant first-order sidebands of the VCSEL.

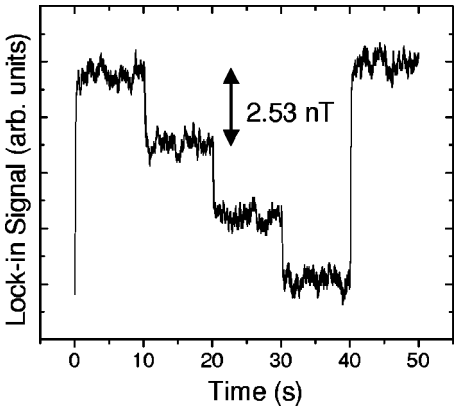

FIG. 3. The lock-in signal is plotted as a function of time as the magnetic flux is stepped in 10 s intervals. The lock-in time constant is 30 ms with a filter roll off 24 dB/octave. The magnetic flux density during the measurement is nominally 73.9 μT.

CPT resonance.[8,11] The energy difference between two Zeeman states in the $F=1$ and $F=2$ hyperfine manifolds at small magnetic flux densities is given approximately by

$$\hbar\omega_{m_1,m_2} \approx \hbar\omega_{0,0} + (m_1 + m_2)\gamma B, \tag{1}$$

where $\hbar\omega_{0,0}$ is the energy difference between the magnetically insensitive states $|F=1,m_1=0\rangle$ and $|F=2,m_2=0\rangle$, m_1 and m_2 are, respectively, the azimuthal quantum numbers for the $F=1$ and $F=2$ states, γ is the gyromagnetic ratio of the atom, and B is the magnitude of the magnetic flux density. Thus, the CPT magnetometer is a scalar detector, but can be operated as a vector magnetometer, sensitive to a magnetic field along a single spatial coordinate, by applying a bias field along the direction of measurement.

To excite the CPT resonance, we tune the VCSEL to the D1 line of ^{87}Rb at 795 nm. A local oscillator modulates the current to the VCSEL at 3.4 GHz, one-half of the hyperfine splitting of the Rb ground state, creating two first-order sidebands that are simultaneously resonant with the two hyperfine ground states to the $P_{1/2}$ excited state [Fig. 2(b)].[12] When the frequency difference between the first-order sidebands is equal to the splitting between two Zeeman states, the atoms are optically pumped into a coherent dark state. We then observe a reduction of the absorbed light power, for example, by 5.4% when the current modulation frequency is tuned to the $|1,-1\rangle-|2,-1\rangle$ resonance.

To operate the magnetometer, the frequency of two different hyperfine transitions must be measured to subtract the $\omega_{0,0}$ contribution to Eq. (1). Typically, $\omega_{0,0}$ is measured once to calibrate the magnetometer for performing a series of magnetic field measurements using a magnetically sensitive transition. In general, $\omega_{0,0}$ differs from the unperturbed atomic ground-state splitting mainly because of the buffer-gas shift, which is temperature dependent and requires periodic calibration.[13] Other shifts include a second-order magnetic field shift and a light shift due to both the resonant and off-resonant sidebands. The magnetometer achieves maximal sensitivity in a magnetic field that is either parallel or transverse to the light propagation direction. For convenience, we operate with a parallel field, and thus selection rules allow CPT resonances to form only when $m_1-m_2=0$. We use the $|1,-1\rangle-|2,-1\rangle$ resonance because optical pumping preferentially populates the negative-m Zeeman states making the amplitude of the $|1,-1\rangle-|2,-1\rangle$ resonance a factor of 2.0 larger than the $|1,1\rangle-|2,1\rangle$ resonance. When the magnetometer is in operation, the frequency of the local oscillator is tuned to approximately $\omega_{-1,-1}$. We frequency modulate the local oscillator frequency at 3.9 kHz to enable phase-sensitive detection of the CPT resonance [Fig. 2(a)]. The resulting signal from the lock-in amplifier is shown in Fig. 3, where the magnetic flux density has been changed in 2.5 nT steps.

To achieve small size, low-power consumption, and to keep alkali metal off the cell windows, the heat sources (the ITO heaters) for the vapor cell are located as close to the windows as possible. However, the currents passing though the ITO heaters and a thermoelectric element (used to temperature stabilize the base plate on which the magnetic sensor sits) create a significant field gradient across the cell. This drastically broadens the $|1,-1\rangle-|2,-1\rangle$ resonance to 520 kHz, compared to 11.5 kHz for the magnetically insensitive $|1,0\rangle-|2,0\rangle$ resonance. To eliminate the effects of the gradients, we chop the currents through the ITO heaters and the thermoelectric element. When the currents are off, we measure the magnetic flux density using a CPT resonance that is 13.2 kHz wide. The currents are chopped at 40 Hz with a duty cycle of 50%, and a sample-and-hold circuit is placed after the photodiode amplifier that samples the signal with a measurement duty cycle of 39.5%. The reduction in measurement time only degrades the sensitivity by a factor of 1.6.

Figure 4 shows the noise spectrum of the CPT signal when the lock-in time constant is 1 ms. The demodulation frequency of the local oscillator is chosen to be 3.9 kHz, a half-integer harmonic of 40 Hz. Thus, the phase of the demodulation frequency is reversed at the start of each measurement cycle giving rise to the 20 Hz peak in the lock-in noise spectrum. This eliminates a systematic error that would result from starting the measurement cycle at constant demodulation phase by using an integer harmonic. To suppress the 20 Hz peak, a magnetic flux density measurement as in Fig. 3 is performed with a time constant of 30 ms and a low-pass roll off of 24 dB/octave.

The sensitivity of the magnetometer is determined by the detector noise voltage density, to which there are two roughly equal contributions: The laser amplitude (AM) noise and the shot noise from the detected photocurrent. Roughly one-half of the photocurrent is dark current caused by the

Downloaded 30 Dec 2004 to 132.163.52.165. Redistribution subject to AIP license or copyright, see http://apl.aip.org/apl/copyright.jsp

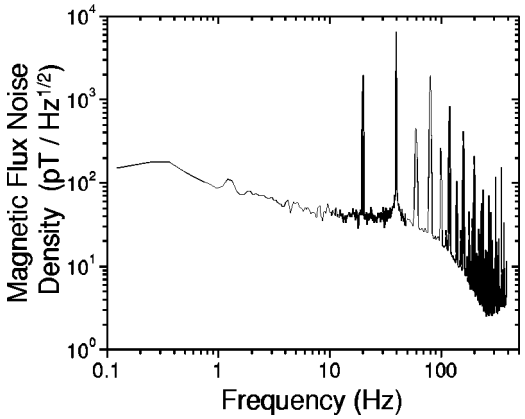

FIG. 4. Power spectral density of the lock-in signal converted to units of magnetic flux density. The lock-in time constant is 1 ms with a filter roll off 24 dB/octave.

photodiode being in direct thermal contact with the cell, which is heated to 120 °C. Other minor contributors to the noise are laser frequency to amplitude (FM–AM) conversion noise and electronic noise. The measured sensitivity of the magnetic sensor is 50 pT $Hz^{-1/2}$ at 10 Hz bandwidth (Fig. 4).

The present result clearly demonstrates that atom-optical magnetometers with millimeter dimensions can provide excellent performance. However, many aspects of the current magnetic sensor are not optimal, and in future devices we can both improve the sensitivity and reduce the power consumption. Optimization of the VCSEL design and optics will improve the sensitivity by providing a more uniform light intensity distribution within the cell and reducing the VCSEL-related noise sources. The present sensor uses 195 mW of power, which can be reduced significantly by improving the microwave modulation efficiency of the VSCEL and redesigning the thermal isolation of the cell. Ultimately, the shot-noise-limited sensitivity of a CPT-based magnetic sensor will be 1 pT $Hz^{-1/2}$, while the power consumption can be reduced to less than 25 mW. We believe that an entire CPT magnetometer, including a 3.4 GHz oscillator and several control circuits, could be assembled that would dissipate <50 mW of power and have a volume of only 1 cm^3.

The fundamental atom shot-noise-limited sensitivity for a 1 mm^3 cell is ~ 0.05 pT $Hz^{-1/2}$ when limited by spin exchange collisions.[14] To approach this sensitivity, it will be advantageous to implement a magnetometry scheme where the Zeeman splitting is measured directly. One such method amenable to miniaturization has been proposed by Budker *et al.*,[15] in which light modulated at a harmonic of the Larmor frequency induces a nonlinear magneto-optical rotation resonance observable at high magnetic fields. The advantages of this method are several. The spin decoherence time for Zeeman states is typically longer than the hyperfine decoherence time.[16] Use of a balanced polarimeter to detect the optical rotation can eliminate much of the AM and FM–AM noise from the VCSEL. Additionally, measuring the Larmor frequency directly eliminates the need to calibrate the magnetically insensitive microwave transition, and small oscillators that operate at the lower Larmor frequency consume less power and are readily available.

In conclusion, we have demonstrated CPT-based magnetometry in a structure of only 12 mm^3, which is smaller by several orders of magnitude than current state-of-the-art optical magnetometers. The magnetic sensor demonstrates the integration of a micromachined vapor cell, micro-optics, and a semiconductor laser and detector into a compact package with a sensitivity of 50 pT $Hz^{-1/2}$. A complete magnetometer with a volume of 1 cm^3 using only 50 mW of power appears feasible by including miniaturized control electronics and a gigahertz local oscillator. Further improvements in sensitivity and power consumption are attainable by implementing a magnetometer where the Larmor frequency is measured directly. The use of wafer-level fabrication of components and batch fabrication techniques should enable low-cost mass production of the optical magnetometers, thereby drastically reducing manufacturing costs.

The authors gratefully acknowledge valuable advice from H. G. Robinson. This work was supported by the Microsystems Technology Office of the U.S. Defense Advanced Research Projects Agency (DARPA). This work is a contribution of NIST, an agency of the U.S. government, and is not subject to copyright.

[1] T. R. Clem, Naval Eng. J. **110**, 139 (1998).
[2] B. S. P. Sarma, B. K. Verma, and S. V. Satyanarayana, Geophysics **64**, 1735 (1999).
[3] M. N. Livanov, A. N. Kozlov, S. E. Sinelnikova, J. A. Kholodov, V. P. Markin, A. M. Gorbach, and A. V. Korinewsky, Adv. Cardiol. **28**, 78 (1981); G. Bison, R. Wynands, and A. Weis, Appl. Phys. B: Lasers Opt. **76**, 325 (2003).
[4] H. G. Dehmelt, Phys. Rev. **105**, 1924 (1957).
[5] I. K. Kominis, T. W. Kornack, J. C. Allred, and M. V. Romalis, Nature (London) **422**, 596 (2003).
[6] D. Budker, D. F. Kimball, S. M. Rochster, V. V. Yashchuk, and M. Zolotorev, Phys. Rev. A **62**, 043403 (2000).
[7] H. Weinstock, (ed.), *SQUID Sensors: Fundamentals, Fabrication, and Applications* (Kluwer Academic, Dordrecht, 1996).
[8] M. Stahler, S. Knappe, C. Affolderbach, W. Kemp, and R. Wynands, Europhys. Lett. **54**, 323 (2001).
[9] S. Knappe, V. Shah, P. D. D. Schwindt, L. Hollberg, J. Kitching, L.-A. Liew, and J. Moreland, Appl. Phys. Lett. **85**, 1460 (2004).
[10] L.-A. Liew, S. Knappe, J. Moreland, H. Robinson, L. Hollberg, and J. Kitching, Appl. Phys. Lett. **84**, 2694 (2004).
[11] E. Arimondo, Prog. Opt. **35**, 257 (1996).
[12] J. Kitching, S. Knappe, N. Vukicevic, L. Hollberg, R. Wynands, and W. Weidmann, IEEE Trans. Instrum. Meas. **49**, 1313 (2000).
[13] J. Vanier and C. Audoin, *The Quantum Physics of Atomic Frequency Standards* (Hilger, London 1989).
[14] J. C. Allred, R. N. Lyman, T. W. Kornack, and M. V. Romalis, Phys. Rev. Lett. **89**, 130801 (2002).
[15] D. Budker, D. F. Kimball, V. V. Yashchuk, and M. Zolotorev, Phys. Rev. A **65**, 055403 (2002).
[16] Y.-Y. Jau, A. B. Post, N. N. Kuzma, A. M. Braun, M. V. Romalis, and W. Happer, Phys. Rev. Lett. **92**, 110801 (2004).

Downloaded 30 Dec 2004 to 132.163.52.165. Redistribution subject to AIP license or copyright, see http://apl.aip.org/apl/copyright.jsp